

Applicability of Self-Consistent Mean-Field Theory

Lu Guo,¹ Fumihiko Sakata,² and En-guang Zhao³

¹Department of Mathematical Sciences, Ibaraki University, Mito 310-8512, Ibaraki, Japan

²Institute of Applied Beam Science, Graduate School of Science and Engineering, Ibaraki University, Mito 310-8512, Ibaraki, Japan

³Institute of Theoretical Physics, Chinese Academy of Sciences, Beijing 100080, China

(Dated: October 16, 2019)

Within the constrained Hartree-Fock (CHF) theory, an analytic condition is derived to estimate whether a concept of the self-consistent mean-field is realized or not in level repulsive region. The derived condition states that an iterative calculation of CHF equation does not converge when the quantum fluctuations coming from two-body residual interaction and quadrupole deformation become larger than a single-particle energy difference between two avoided crossing orbits. By means of the numerical calculation, it is shown that the analytic condition works well for a realistic case.

PACS numbers: 21.60.Jz, 21.10.Pc, 21.30.Fe

I. INTRODUCTION

The Hartree-Fock mean-field theory has been applied for various quantum many-fermion systems successfully. Violating various conservation laws satisfied by the Hamiltonian, one obtains such an appropriate mean-field that could incorporate various correlations of the system as much as possible. Its many important theoretical concepts like a stability of the mean-field, an appearance of massless collective motion in association with restoration dynamics of broken symmetries, etc constitute an outstanding virtue of the self-consistent mean-field theory. Here it should be noticed that the mean-field is characterized by various averaged quantities, which express an amount of symmetry breaking like a shape deformation in the coordinate space or a gauge deformation in the quasi-spin (pairing) space. These averaged quantities as well as a concept of mean-field are expected to have physical reality only when the many-body system under consideration is near stationary, at least locally homogeneous, and well isolated from the other local minimum. At the best of our knowledge, there has been no discussion on when a concept of the self-consistent mean-field is realized, how and why it breaks down. When a couple of single-particle (sp.) states just below and above the Fermi surface comes close with each other, one may expect that there locates another mean-field near to the lowest one. In this paper, we will discuss to what extent the self-consistent one-body potential has a sense, when two orbits around the Fermi surface interact with each other.

Theoretically, an avoided crossing occurs rather frequently in various fields of physics like the molecular, atomic, biological systems, as well as the quantum dot and atomic nuclear systems [1, 2, 3, 4]. In a development of the nuclear structure physics, there have been many discussions on an applicability of the cranked mean-field theory near avoided level crossing region [5], where large angular momentum fluctuations and spurious interactions between two crossing orbits have been explored. An argument for removing a certain spurious interaction and

for introducing a set of diabatic sp. states in the cranked mean-field [6, 7, 8, 9, 10, 11] seems to be reasonable, because the angular momentum is a constant of motion and the interaction between different rotational bands should act at a given angular momentum rather than at a given rotational frequency. However, these treatments seem to be still in a phenomenological stage.

The above argument may not be simply extended to deformation constrained mean-field theory. In this case, an interaction between two potential energy surfaces (PESs) with different quadrupole deformation may not necessarily be regarded as spurious, because the Hamiltonian and quadrupole operator do not commute with each other. Interestingly, it has been suggested that the pairing interaction between two orbits locating below and above the Fermi surface, and having spherical and deformed shape, might be spurious in the level crossing region [6]. By eliminating the spurious interactions and comparing with experiments, very interesting conclusions have been deduced like "a flat PES does not automatically lead to large fluctuation of the shape". However, there still remains a decisive question how the above statement is justified from the underlying dynamics.

To understand how the mean-field changes by itself when it acquires additional deformation, and to study more deeply what actually happens in the self-consistent mean-field near the level crossing region from the underlying microscopic dynamics, a rather heavy numerical method called the configuration dictated CHF method [12] has been developed. Applying this method to realistic cases, one may get many PESs which are approximately characterized by the sp. configurations relative to the lowest PES [13]. As pointed out in our previous papers [13, 14], the CHF iterative calculation sometimes meets a difficulty of poor convergence or even non-convergence near the level repulsive region, no matter how much efforts one makes to get convergence.

In this paper, we will explore how a competition between the mean-field and the quantum fluctuations coming from two-body residual interaction and quadrupole deformation plays a decisive role in breaking the concept

of self-consistent mean-field near level repulsive region.

II. THEORETICAL METHOD

The nuclear Hamiltonian is given by

$$\hat{H} = \sum_{i=1}^N \left[t_i + c^y_i c_i + \frac{1}{4} \sum_{i,j}^N v_{ij} c^y_i c^y_j c_i c_j \right]; \quad (1)$$

where t_i is the kinetic energy, and v_{ij} the anti-symmetrized effective two-body interaction. Here and hereafter, \hat{c}_i , \hat{c}_i^\dagger are used to denote numerical basis. To define the self-consistent HF state $j(\mathbf{q})i$ with a given quadrupole moment \mathbf{q} , one applies the deformation CHF method. In the minimization process, one introduces Lagrange multipliers to obtain the Slater determinant wave function $j(\mathbf{q})i$ through the CHF variational equation

$$\begin{aligned} h(\mathbf{q})j\hat{H}j(\mathbf{q})i + \frac{1}{2}w h(\mathbf{q})j\hat{Q}_{20}j(\mathbf{q})i \\ + \frac{1}{2} \sum_{i,j}^N h(\mathbf{q})\hat{x}j(\mathbf{q})i = 0; \end{aligned} \quad (2)$$

with constraints

$$h(\mathbf{q})j\hat{Q}_{20}j(\mathbf{q})i = \mathbf{q}; \quad (3)$$

$$h(\mathbf{q})\hat{x}j(\mathbf{q})i = 0; \quad (4)$$

where \hat{x} denotes a center of mass coordinate. In our numerical calculation of solving the CHF equation, three dimensional harmonic oscillator basis is used, and the Gogny D1S interaction [15, 16, 17, 18, 19, 20], the Coulomb force and the center of mass motion up to the exchange terms are taken into account. A quadratic constraint of quadrupole moment is used to treat concave areas of the PES. In Eq.(2), w denotes an input parameter which allows us to vary an expectation value $h(\mathbf{q})j\hat{Q}_{20}j(\mathbf{q})i$. Meaning of parabola width w was discussed in Ref. [21], and is chosen to be 1.0×10^{-3} [MeV fm⁻²] in our calculation. The Lagrange multiplier (\mathbf{q}) is given by

$$(\mathbf{q}) = w h(\mathbf{q})j\hat{Q}_{20}j(\mathbf{q})i; \quad (5)$$

and an effective value of (\mathbf{q}) is allowed to change during the iterations. The symmetries $\hat{P}e^{i\hat{J}_z}$ (z-simplex) and $\hat{P}e^{i\hat{J}_y} \wedge (\hat{S}_y^\dagger)$ [22, 23] are imposed in our numerical calculation, where \hat{P} is the parity operator, $e^{i\hat{J}_i}$ the rotation operator around i axis by an angle θ , and \wedge the time reversal operator. Due to the z-simplex and \hat{S}_y^\dagger symmetries, a mass asymmetry of the nucleus is allowed only along the x axis. To keep the center of mass motion fixed, we impose a quadratic constraint in the x-axis direction with Lagrange multiplier

$$0 = \sum_i h(\mathbf{q})\hat{x}j(\mathbf{q})i; \quad (6)$$

and take $w = 1.0 \times 10^{-4}$ [MeV fm⁻²] in our numerical calculation.

For convenience, the constrained Hamiltonian is denoted by $\hat{C} = \hat{H} - \hat{Q}_{20} + \hat{Q}_0$. Having solved the CHF equation (2), one obtains a set of sp. energies $f_k(\mathbf{q})g$ as well as the sp. states $f'_{-k}(\mathbf{q})g$. The constrained Hamiltonian is then expressed as

$$\begin{aligned} \hat{C}(\mathbf{q}) = E_0(\mathbf{q}) + \sum_{i=1}^N (c_i^\dagger c_i + c_i c_i^\dagger) \\ + \sum_{i=1}^N (c_i^\dagger c_i) c_i^\dagger c_i + :C(\mathbf{q}):; \end{aligned} \quad (7)$$

where c_i^\dagger and c_i are particle- and hole-creation operators satisfying

$$c_i^\dagger c_i j(\mathbf{q})i = c_i^\dagger c_i^\dagger j(\mathbf{q})i = 0; \quad (8)$$

Here and hereafter, the particle states are denoted by j , and hole states by i ; j . The letters k, l are used when no distinction is needed. The operator $:C(\mathbf{q}):$ denotes the two-body residual interaction consisting of the normal-ordered product of four fermions with respect to $j(\mathbf{q})i$ in the two-body interaction

$$:C(\mathbf{q}): = \frac{1}{4} \sum_{k_1 k_2 k_3 k_4}^X v_{k_1 k_2 k_3 k_4} N(c_{k_1}^\dagger c_{k_2}^\dagger c_{k_3} c_{k_4}); \quad (9)$$

With the aid of the sp. states $f'_{-k}(\mathbf{q})g$, the CHF energy $E_0(\mathbf{q})$ is given by

$$\begin{aligned} E_0(\mathbf{q}) = h(\mathbf{q})j\hat{C}(\mathbf{q})j(\mathbf{q})i \\ = \sum_i (t_{ii} - (\mathbf{q})Q_{ii}) + \frac{1}{2} \sum_{i,j}^X v_{ij}ij + E_{cm}; \end{aligned} \quad (10)$$

where

$$E_{cm} := \frac{\hbar P_{cm}^2}{2Nm}; \quad (11)$$

is the center of mass energy with total momentum P_{cm} .

The quadrupole operator is expressed as

$$\begin{aligned} \hat{Q}_{20} = \mathbf{q} + \sum_i f Q_{-i}(\mathbf{q}) c_i^\dagger c_i + h.c.g \\ + \sum_i Q_{-i}(\mathbf{q}) c_i^\dagger c_i \sum_{ij}^X Q_{ij}(\mathbf{q}) c_j^\dagger c_j c_i^\dagger c_i; \end{aligned} \quad (12)$$

where h.c. denotes the Hermitian-conjugation of the former term, and \mathbf{q} is the quadrupole deformation of the system given by

$$\mathbf{q} = \sum_i Q_{ii}(\mathbf{q}); \quad (13)$$

The deformation-dependent particle-hole component $Q_{-1}(q)$ gives an information on deformation fluctuation.

To understand how the CHF state undergoes a structure change depending on the quadrupole deformation, it is desirable to obtain $j_{-1}(q+q_i)$ in such a way that it can be regarded as a smooth function of q . For this aim, we apply the configuration dictated CHF method, which is briefly recapitulated below. Let $j_{-1}(q_i)$ be a known CHF state satisfying condition $h_{-1}(q)j_{-1}Q_{20}j_{-1}(q_i) = q_i$. To find a new CHF state $j_{-1}(q+q_i)$ which is supposed to be continuously connected with $j_{-1}(q_i)$, we exploit the following condition

$$\lim_{q \rightarrow 0} h_{-1}(q)j_{-1}(q+q_i) = j_{-1}(q_i); \quad (14)$$

where $j_{-1}(q)$ denotes a set of occupied wave functions constructing the single Slater determinant $j_{-1}(q_i)$. That is, a small increment q is numerically adjusted by the maximum overlap criterion in Eq. (14) under a given accuracy, so as to maintain a characteristic property of the CHF state. In our calculation, q is so determined as to fulfill the condition

$$j_{-1}(q)j_{-1}(q+q_i)j_{-1}^2 > 0.9; \quad (15)$$

In this way, the configuration specifying $j_{-1}(q_i)$ is kept continuously as a function of q . Since the CHF state at $q+q_i$ is dictated by the configuration of the preceding CHF state at q , this method is called the configuration dictated CHF method. It can also be generalized to get the excited HF states and the continuously-connected PESs. Applications of the configuration dictated CHFB method in the levelcrossing region as well as in the shape coexistence phenomena, with and without the pairing effect have been reported elsewhere [13].

In our numerical calculation, a convergence condition is given as

$$X_k^{(n)}(q) - X_k^{(n-1)}(q) < 10 \text{ eV}; \quad (16)$$

where $X_k^{(n)}$ denotes the sp. energies in the n -th iteration.

III. FRAGILITY OF MEAN-FIELD

A. difficulty of non-convergence near level repulsive region in CHF theory

In our calculation, the sp. wave functions are expanded in three-dimensional harmonic oscillator basis up to the principal quantum number $N_0 = 8$. The ground state of ^{66}Se is obtained after having optimized triaxial deformation parameters of the Hermite polynomials. The optimized range parameters thus obtained include some effects of higher major shells. Note that, no optimization has been done in the most HF and HFB calculations [24, 25, 26, 27], although a larger configuration space is

TABLE I: The optimized ground state properties of ^{66}Se . The binding energy (BE), quadrupole deformation parameter (β_2) and triaxial deformation (γ) are listed. The experimental data is cited from Ref. [28].

| | HF | HFB | Exp. |
|-----------|---------|---------|---------|
| BE [MeV] | 544.502 | 545.623 | 547.827 |
| β_2 | 0.241 | 0.234 | |
| (degree) | 47.256 | 59.541 | |

adopted. It is well known that the optimum parameters change depending on the number of major shell, and become rather stable as the number increases [21]. In order to examine a reliability of the optimized configuration space, the ground state properties of ^{66}Se both in HF and HFB calculations are listed in Table I, together with the experimental binding energy [28]. The binding energies in both calculations reproduce the experimental data well, though the total binding energy in the HFB is about 1.1 MeV lower than that in the HF calculation. A comparison between the HF and HFB calculations in Tab. I indicates that the nuclear deformation becomes small (favors the spherical shape) when one includes the pairing correlation into the mean-field. In the following discussion, the number of major shell used in our calculation may not have decisive importance.

Starting from the ground state, the quadratic CHF calculation with the configuration dictated method is carried out in such a small step as the solutions are considered to be a continuous function of the deformation. Such a point-by-point heavy calculation is needed for discussing the dynamical structure change of nuclear system. In numerically obtaining the PES, the same range parameters as those in the ground state are used to trace an evolution of the ground state configuration as a function of deformation, which makes the sp. level crossing dynamics transparent. Figure 1 shows (a) the quadrupole moment as a function of q , and (b) the lowest PES for ^{66}Se . One may observe that both the quadrupole deformation and PES change smoothly, except for a missing region around $q = 150 \text{ fm}^2$. When the constrained quadrupole moment is decreased by a small amount q from a critical point at $q_0 = 177.365 \text{ fm}^2$, the CHF iteration meets a difficulty of non-convergence no matter how much efforts one makes to get convergence. After the missing region, the continuously-connected PES passing through an excited local minimum ($q = 100 \text{ fm}^2$) is obtained.

The nonlinear CHF equation is solved in an iterative way until the CHF Hamiltonian $h(q)$ and density $\rho(q)$ are diagonalized simultaneously [$[h(q), \rho(q)] = 0$]. In the numerical basis, the sp. wave function $\psi_k^{(n)}(q)$ at the n -th iteration is expressed as $\psi_k^{(n)}(q)$, and $\rho^{(n)}(q)$ and

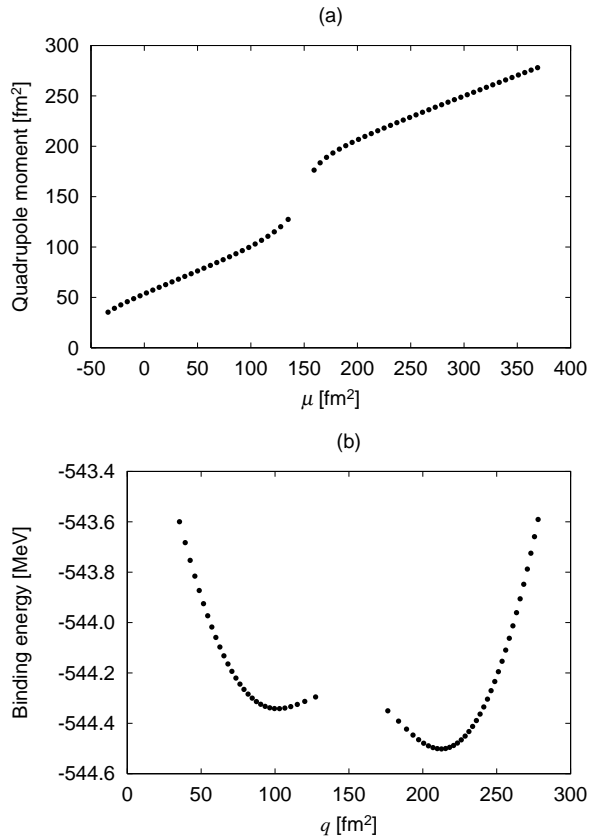


FIG. 1: CHF calculation for ^{66}Se : (a) the calculated quadrupole moment as a function of input quadrupole moment parameter μ ; (b) binding energy as a function of quadrupole moment q .

$h^{(n)}(q)$ are given as

$$\begin{aligned} h^{(n)}(q) &= \sum_i^{X} f_i^{(n-1)}(q) f_i^{(n-1)}(q); \\ h^{(n)}(q) &= t^{(n)}(q) + v^{(n)}(q) Q^{(n)}(q); \\ h^{(n)}(q) &= w^{(n)}(q); \end{aligned} \quad (17)$$

Here $t^{(n)}(q)$ denotes the HF potential, and

$$w^{(n)}(q) = h^{(n-1)}(q) \hat{D}_{20} j^{(n-1)}(q) i; \quad (18)$$

where $j^{(n-1)}(q)i$ is the Slater determinant constructed by $f_i^{(n-1)}(q)g$.

On a way to convergence, expectation values of one-body density $t^{(n)}(q)$ in a representation of using $f_k^{(n)}(q)g$, i.e.,

$$t^{(n)}(q) = \sum_k^{X} f_k^{(n)}(q) f_k^{(n)}(q); \quad (19)$$

with respect to the hole and particle states are supposed to gradually reach 1 and 0, respectively. To understand

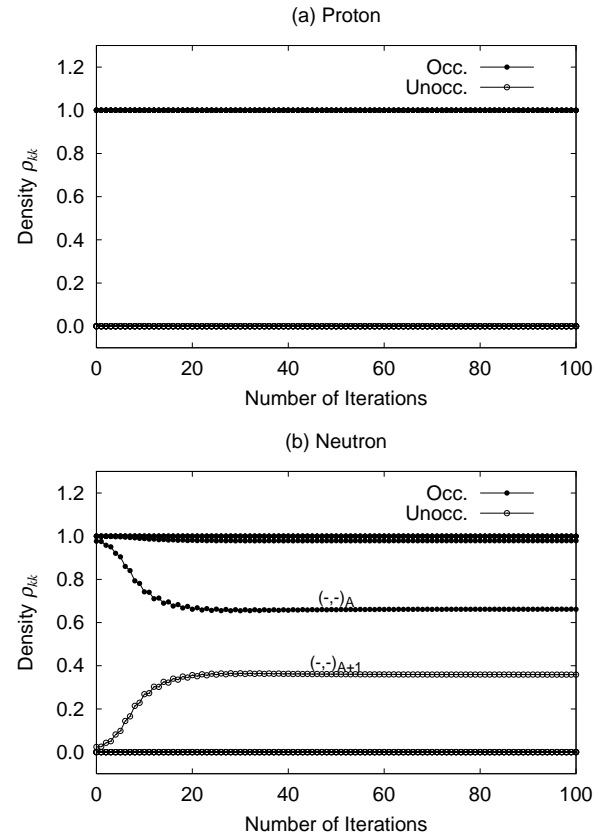


FIG. 2: Diagonal components of (a) proton and (b) neutron density as a function of number of iteration for a non-convergent case with $q = 150$ fm². The single-particle basis where h is diagonal is used. Occ. and Unocc. stand for occupied and unoccupied orbits, respectively. $(-,-)$ denotes the parity and signature, and its subscripts A and $A+1$ represent the orbits responsible for the non-convergent difficulty.

what prevents the CHF iterative calculation from convergence, Fig. 2 depicts the diagonal components of proton and neutron densities as a function of number of iterations, for a case of non-convergence with $q = 150$ fm² (see Fig. 1(a)). In the case of non-convergence, the quadrupole deformation parameter q is used in replace of q . One may observe that the expectation values of proton density for the unoccupied orbits converge to 0, while those for occupied orbits to 1. For the case of neutron, there appears a similar situation for the most single-hole and single-particle states, except for two specific orbits labeled as $(-,-)_A$ and $(-,-)_{A+1}$. Here, A denotes the number of neutron occupied orbits, and the sp. states are specified by the parity and signature quantum numbers $(-,-)$, since the asymptotic Nilsson quantum numbers are not good quantum numbers when the reaction symmetry is lost. For convenience, a subscript A and $A+1$ for $(-,-)$ is introduced to identify the occupied and unoccupied orbits responsible for the difficulty of non-convergence. As seen from Fig. 3, these two specific neutron orbits with opposite quadrupole moments,

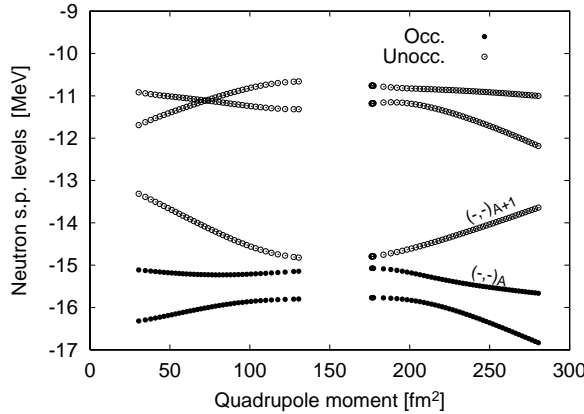


FIG. 3: Neutron single-particle energies near the Fermi surface. O_{cc} and U_{nocc} stand for occupied and unoccupied orbits, respectively. The symbol is same as that in Fig. 2.

i.e., one is of deformation driving and the other of anti-driving, lying just below and above the Fermi surface are interacting. One may expect that the two specific orbits $(\ ; \)_A$ and $(\ ; \)_{A+1}$ play a dominant role in preventing the CHF calculation from convergence.

To exhibit crucial effects of two neutron orbits on the non-convergence property in the CHF calculation, an absolute value of off-diagonal CHF Hamiltonian $\tilde{H}_{A,A+1}^{(n)}$ and a difference of diagonal components $\tilde{H}_{A+1,A+1}^{(n)} - \tilde{H}_{A,A}^{(n)}$ for the case with $\lambda = 150.0 \text{ fm}^{-2}$ are shown in Fig. 4 as a function of number of iterations. Here, the CHF Hamiltonian is expressed in a representation where density matrix $^{(n)}$ is diagonal, i.e.,

$$\tilde{h}_{kl}^{(n)}(q) \stackrel{X}{\longrightarrow} \sum_{k=1}^{n-1} (q) h^{(n)}(q) \sum_{l=1}^{n-1} (q) : \quad (20)$$

In the C HF theory, it is usual to employ the above representation where the n -th quantities are entirely expressed in terms of the $(n-1)$ th sp. wave function $f'_{k^{(n-1)}} g$.

In a case of convergence, the off-diagonal component of the CHF Hamiltonian would become smaller, and finally reach to 0, as the number of iteration increases. In the present non-convergent case, there appears a staggering property both in the diagonal and off-diagonal components. During the iteration, $\mathfrak{H}_{A,A+1}^{(n)}$ increases first, and then starts to oscillate around some central value. In this case, the off-diagonal component always remains and never reaches to 0, rather than being included into the mean-field. Figure 4 indicates that the two interacting orbits make it difficult to apply the CHF mean-field theory.

B. microscopic dynamics of non-convergence

In this subsection, it is discussed how the non-convergent difficulty and the staggering property appear

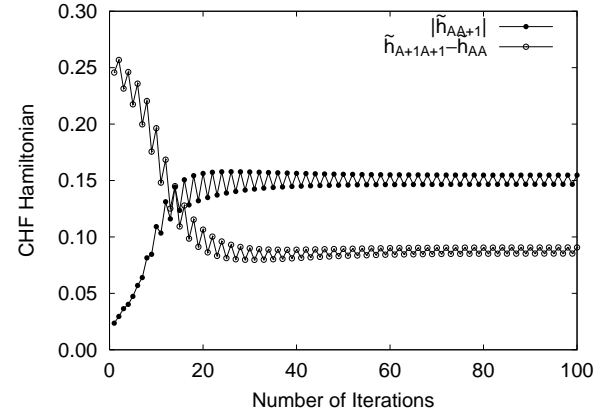


FIG. 4: The absolute value of off-diagonal component and the difference of diagonal components of the CHF Hamiltonian between two specific orbits as a function of number of iteration for the non-convergent case with $\hbar = 150.0 \text{ fm}^2$. A representation of using sp. basis where density $^{(n)}$ is diagonal is used.

as a result of the microscopic dynamics. Namely, it is explored whether or not one gets a convergent CHF state at $q = q_0$ (q a corresponding deformation parameter = 0), when there exists a convergent CHF state $j(q_0)i$ at $q = q_0$ with corresponding set of self-consistent sp. states $f_k(q_0); k(q_0)g$. Since the CHF state $j(q_0)i$ is used as an initial trial wave function to proceed the iterative calculation at $q = q_0$ (q , there hold the following relations

$$h^{(0)}(q_0 - q) = h(q_0);$$

$${}'^{(0)}_k(q_0 - q) = {}'{}_k(q_0); \quad (21)$$

In order to study dynamical change of the sp. wave functions during the iterations, it turns out to be preferable to use a \vec{q} -xed representation, ie., the \vec{q} -representation of using the CHF sp. states $f'_{\vec{k}}(\vec{q}_0)g$, rather than the usual representation of using n -dependent sp. wave functions $f'_{\vec{k}}^{(n-1)}(\vec{q}_0 - \vec{q})g$ like in Eq. (20). The n th Hamiltonian in the \vec{q} -representation is expressed as

where the matrix elements of kinetic energy, deformation operator and the HF potential in the q_0 -representation

are defined as

$$\begin{aligned} t_{k1} &= \sum_{i=1}^X \langle_{k1}(q_0) t_{i1}(q_0); \\ Q_{k1} &= \sum_{i=1}^X \langle_{k1}(q_0) Q_{i1}(q_0); \\ \langle_{k1}^{(n)}(q_0, q) &= \sum_{i=1}^X \langle_{k1}(q_0) \langle_{i1}^{(n)}(q_0, q) t_{i1}(q_0); \end{aligned} \quad (23)$$

and

$$\begin{aligned} \langle_{k1}^{(n)}(q_0, q) &= w \langle_{00}(q_0, q) + \\ h^{(n-1)}(q_0, q) j \hat{Q}_{20} j^{(n-1)}(q_0, q) i; \\ (\text{for } n \neq 0); \\ \langle_{k1}^{(0)}(q_0, q) &= \langle_{00}(q_0) = w \langle_{00}(q_0) j \hat{Q}_{20} j(q_0) i; \\ (\text{for } n = 0); \end{aligned} \quad (24)$$

Making the following analytic understanding on our numerical results transparent and simple, we exploit such an approximate expression, i.e.,

$$\sum_{i=1}^{X-1} \langle_{i1}(q_0) \langle_{i1}(q_0) = \sum_{i=1}^{X-1} \langle_{i1}^{(n)}(q_0, q) \langle_{i1}^{(n)}(q_0, q); \quad (25)$$

which states that a contribution to the mean-field from the lowest ($A - 1$) number of hole-states is independent of small deformation change as well as number of iteration n . It turns out that Eq. (25) is well justified in our numerical calculation discussed in the previous subsection. Employing the above simplification, one may explore the non-convergent dynamics governing the CHF iterative calculation in terms of a 2 2 truncated CHF Hamiltonian expressed as

$$\begin{aligned} \langle_{A,A}^{(n)}(q_0, q) &= \langle_{A,A+1}^{(n)}(q_0, q) \\ \langle_{A+1,A}^{(n)}(q_0, q) &= \langle_{A+1,A+1}^{(n)}(q_0, q); \end{aligned} \quad ! \quad (26)$$

Although a set of eigen states $\langle_{k1}^{(n)}(q_0, q) g$ is numerically obtained by diagonalizing the full CHF Hamiltonian $h^{(n)}(q_0, q)$, the characteristic feature of two interacting orbits is expected to be understood in terms of the truncated 2 2 Hamiltonian in Eq. (26) and 2 2 unitary matrix $U^{(n)}$ given by

$$\begin{aligned} \langle_{A,A}^{(n)}(q_0, q) &= U^{(n)} \langle_{A+1,A}^{(n)}(q_0, q); \\ U^{(n)} &= \begin{pmatrix} a^{(n)} & b^{(n)} \\ c^{(n)} & d^{(n)} \end{pmatrix}; \end{aligned} \quad (27)$$

In accordance with using the q_0 -representation, the above unitary transformation allows us to study the iterative process in terms of a mixing between two fixed states $\langle_{A,A}^{(n)}(q_0)$ and $\langle_{A+1,A}^{(n)}(q_0)$ irrespective of n . To explore a decisive role of relative phase between two orbits on the non-convergent difficulty of the CHF iterative calculation, i.e., on the properties of resultant sp. wave functions obtained after having diagonalized $h_{k1}^{(n)}(q_0, q)$, we use four inter-dependent parameters in $U^{(n)}$ rather than a single independent parameter. Mixing parameters $b^{(n)}$ and $d^{(n)}$ ($b^{(n)}^2 = d^{(n)}^2$) are a measure of degree of mixing between the two specific orbits. In each diagonalization, the subscripts A and $A + 1$ are used to assign the sp. states in an energy increasing order satisfying $\langle_{A,A}^{(n)}(q_0, q) < \langle_{A+1,A}^{(n)}(q_0, q)$.

With the aid of Eq. (27) and the approximate expression in Eq. (25), it is easily shown that the Lagrange multiplier $\langle_{k1}^{(n)}(q_0, q)$ in Eq. (24) fulfills the following simple recurrence relation

$$\langle_{k1}^{(n+1)}(q_0, q) = \langle_{k1}^{(n)}(q_0, q) + \langle_{k1}^{(n)}(q_0, q); \quad (\text{for } n \neq 0); \quad (28)$$

where

$$\langle_{k1}^{(n)}(q_0, q) = 2w a^{(n)} b^{(n)} Q_{A,A+1} - w b^{(n)2} f Q_{A+1,A+1} - Q_{A,A} g; \quad (\text{for } n \neq 0) \quad (29)$$

with an initial relation given as

$$\begin{aligned} \langle_{k1}^{(1)}(q_0, q) &= w \langle_{00}(q_0, q) + h^{(0)}(q_0, q) j \hat{Q}_{20} j^{(0)}(q_0, q) i \\ &= \langle_{k1}^{(0)}(q_0, q) w = \langle_{00}(q_0) w; \quad (\text{for } n = 0); \end{aligned} \quad (30)$$

In the same way, one may derive the general expression of the matrix elements of 2 2 truncated CHF Hamiltonian

in Eq. (26) at the $(n + 1)$ th iteration as

$$\begin{aligned}
 h_{A;A+1}^{(n+1)} &= h_{A;A+1}^{(1)} + a^{(n)} b^{(n)} (v_{A+1;A+1} + 2wQ_{A;A+1}^2) + wb^{(n)}^2 Q_{A;A+1} (Q_{A+1;A+1} - Q_{A;A}); \\
 h_{A;A}^{(n+1)} &= h_{A;A}^{(1)} + 2w a^{(n)} b^{(n)} Q_{A;A} Q_{A;A+1} - b^{(n)}^2 v_{A+1;A+1} - w Q_{A;A} (Q_{A+1;A+1} - Q_{A;A}); \\
 h_{A+1;A+1}^{(n+1)} &= h_{A+1;A+1}^{(1)} + 2w a^{(n)} b^{(n)} Q_{A+1;A+1} Q_{A;A+1} + b^{(n)}^2 v_{A+1;A+1} + w Q_{A+1;A+1} (Q_{A+1;A+1} - Q_{A;A});
 \end{aligned} \quad (31)$$

where the anti-symmetrized two-body interaction in the q_0 -representation is defined as

$$X_{k_1 k_2 k_3 k_4} = \langle k_1 (q_0) | k_2 (q_0) v | k_3 (q_0) | k_4 (q_0) \rangle. \quad (32)$$

Here and hereafter, we use a simple notation $h^{(n+1)}$ instead of $h^{(n+1)}(q_0 - q)$ etc, because we are only discussing the CHF iterative process at $q = q_0 - q$. The matrix elements of truncated Hamiltonian $h_{k_1}^{(1)}$ are given as

$$\begin{aligned}
 h_{A;A+1}^{(1)} &= w Q_{A;A+1}; \\
 h_{A;A}^{(1)} &= \langle A (q_0) | w Q_{A;A} \rangle; \\
 h_{A+1;A+1}^{(1)} &= \langle A+1 (q_0) | w Q_{A+1;A+1} \rangle; \quad (33)
 \end{aligned}$$

which are easily derived by using the initial condition in Eq. (21) and initial relations in Eqs. (22), (24) and (30) for the case with $n = 0$. In deriving Eq. (33), a relation

$$\begin{matrix} h_{A;A}^{(0)} & h_{A;A+1}^{(0)} \\ h_{A+1;A}^{(0)} & h_{A+1;A+1}^{(0)} \end{matrix} = \begin{matrix} \langle A (q_0) | & 0 \\ 0 & \langle A+1 (q_0) | \end{matrix}; \quad (34)$$

satisfied by the preceding CHF solution at $q = q_0$ is also used.

With the aid of Eq. (31), one gets the following relations for two successive truncated CHF Hamiltonians $h^{(n)}$ and $h^{(n+1)}$ as,

$$\begin{aligned}
 h_{A;A+1}^{(n+1)} &= h_{A;A+1}^{(n)} + f a^{(n)} b^{(n)} - a^{(n-1)} b^{(n-1)} g f v_{A+1;A+1} + 2wQ_{A;A+1}^2 g \\
 &\quad + w f b^{(n)}^2 - b^{(n-1)}^2 g Q_{A;A+1} (Q_{A+1;A+1} - Q_{A;A}); \\
 h_{A;A}^{(n+1)} &= h_{A;A}^{(n)} + 2w f a^{(n)} b^{(n)} - a^{(n-1)} b^{(n-1)} g Q_{A;A} Q_{A;A+1} \\
 &\quad - f b^{(n)}^2 - b^{(n-1)}^2 g f v_{A+1;A+1} - w Q_{A;A} (Q_{A+1;A+1} - Q_{A;A}) g; \\
 h_{A+1;A+1}^{(n+1)} &= h_{A+1;A+1}^{(n)} + 2w f a^{(n)} b^{(n)} - a^{(n-1)} b^{(n-1)} g Q_{A+1;A+1} Q_{A;A+1} \\
 &\quad + f b^{(n)}^2 - b^{(n-1)}^2 g f v_{A+1;A+1} + w Q_{A+1;A+1} (Q_{A+1;A+1} - Q_{A;A}) g; \quad (35)
 \end{aligned}$$

In the same way, the off-diagonal component of a difference between $h^{(n)}$ and $h^{(n+2)}$ is given as

$$\begin{aligned}
 h_{A;A+1}^{(n+2)} &= h_{A;A+1}^{(n)} + f a^{(n+1)} b^{(n+1)} - a^{(n-1)} b^{(n-1)} g f v_{A+1;A+1} + 2wQ_{A;A+1}^2 g \\
 &\quad + w f b^{(n+1)}^2 - b^{(n-1)}^2 g Q_{A;A+1} (Q_{A+1;A+1} - Q_{A;A}); \quad (36)
 \end{aligned}$$

Since the second term in the r.h.s. of Eq. (35) contains a factor $a^{(n)} b^{(n)}$ whereas the third term a factor $b^{(n)}^2$, the former term is retained in the following discussions owing to the small parameter $b^{(n)}$.

Numerical values of $h_{A;A}^{(n)}$, $h_{A+1;A+1}^{(n)}$ and $h_{A;A+1}^{(n)}$ are shown in Fig. 5(a) for the non-convergent case with $\epsilon = 150 \text{ fm}^2$. From this figure, one may observe that both components exhibit a staggering property around some averaged values. It should also be noticed that the

off-diagonal component $h_{A;A+1}^{(n)}$ changes its sign from iteration to iteration, whereas $h_{A;A}^{(n)} - h_{A+1;A+1}^{(n)}$ is always negative. The latter is easily understood because a couple of states $\langle A (q) | q \rangle$ and $\langle A+1 (q) | q \rangle$ is defined so as to satisfy a relation $\langle A (q_0) | q \rangle < \langle A+1 (q_0) | q \rangle$. According to the perturbation theory of the 2-2 Hamiltonian, a sign of $a^{(n)} b^{(n)}$ for characterizing the lower state $\langle A (q_0) | q \rangle$ is the same as that of $(h_{A;A+1}^{(n)}) = (h_{A;A}^{(n)})$

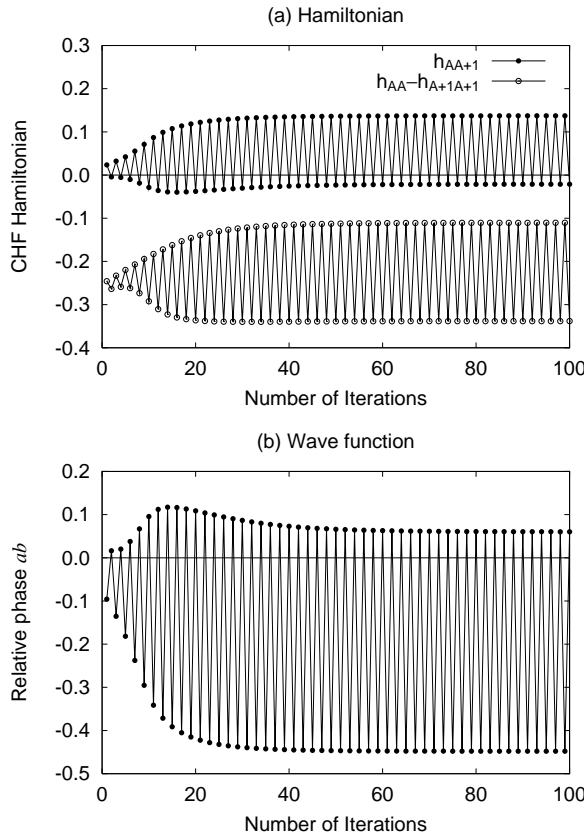


FIG. 5: For the non-convergent case with $\epsilon = 150 \text{ fm}^2$ (a) the off-diagonal Hamiltonian and difference of diagonal components as a function of number of iteration; (b) the relative phase $a^{(n)}b^{(n)}$ of wave function for the orbit $'_{A+1}^{(n)}$.

$h_{A+1,A+1}^{(n)}$). In Fig. 5(b), the numerical value of $a^{(n)}b^{(n)}$ is shown as a function of number of iterations. By comparing Fig. 5(a) with Fig. 5(b), our numerical results are well understood in terms of the above simplified analytic expression in the two dimensional truncated space, and the perturbation theory for the 2-2 Hamiltonian. Since a sign of $a^{(n)}b^{(n)}$ changes from iteration to iteration, it is clear that the higher state $'_{A+1}^{(n)}(q_0 - q)$ and the lower state $'_A^{(n)}(q_0 - q)$ interchange their properties from iteration to iteration.

With the aid of coefficient $a^{(n)}b^{(n)} - a^{(n-1)}b^{(n-1)}$ in the second term of the r.h.s. of Eq. (35), and from the above discussion on different signs between $a^{(n)}b^{(n)}$ and $a^{(n-1)}b^{(n-1)}$, one may understand why $h_{A,A+1}^{(n+1)}$ becomes large. Since there is a coefficient $a^{(n+1)}b^{(n+1)} - a^{(n-1)}b^{(n-1)}$ in the second term of the r.h.s. of Eq. (36), and since the sign of $a^{(n+1)}b^{(n+1)}$ and that of $a^{(n-1)}b^{(n-1)}$ are the same, it is easily recognized why the ph component at $(n+2)$ th iteration becomes small. These equations clearly state that the quantum fluctuations coming from two-body residual interaction and quadrupole deformation become small in one iteration, and become large in the next, forming the staggering property. In

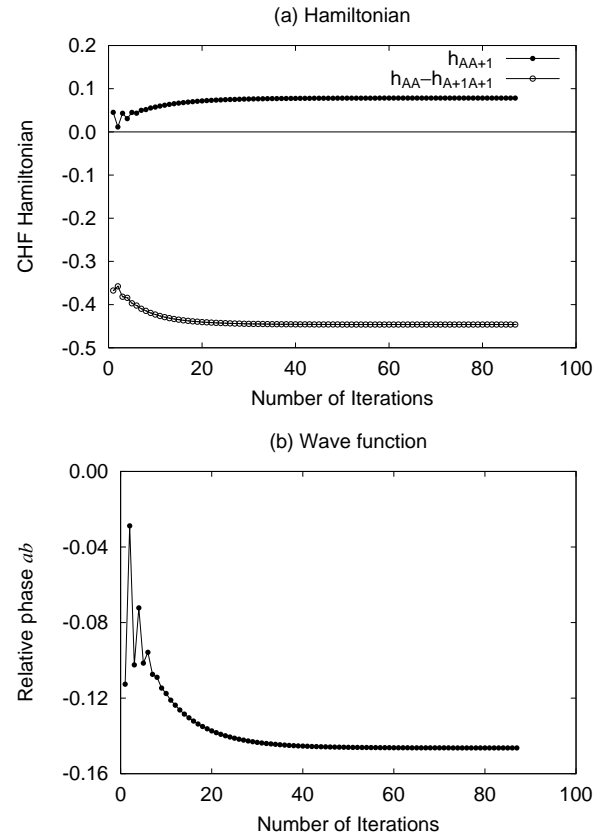


FIG. 6: For the convergent case with $\epsilon = 180 \text{ fm}^2$. Notation is the same as Fig. 5.

other words, the major part of the two-body interaction could not be approximated successfully by the averaged one-body potential when the sign of $a^{(n)}b^{(n)}$ changes from one iteration to the next. Physically one may understand the above situation as follows: two mean-fields, one characterized by occupied $'_A(q_0)$ and the other by occupied $'_{A+1}(q_0)$, interact too strongly by the two-body residual interaction to be approximated by a single mean-field.

In contrast with the non-convergent case, the same quantities for convergent CHF calculation at $\epsilon = 180 \text{ fm}^2$ are shown in Fig. 6. One may observe that the sign of off-diagonal Hamiltonian is kept the same during the iteration, and the sign of $a^{(n)}b^{(n)}$ is always the same during the iteration until the convergence is achieved. Since the sign of $a^{(n)}b^{(n)}$ does not change during the iterations in the case of convergence, the quantum fluctuations characterized by coefficient $a^{(n)}b^{(n)} - a^{(n-1)}b^{(n-1)}$ in Eq. (35) and by $a^{(n+1)}b^{(n+1)} - a^{(n-1)}b^{(n-1)}$ in Eq. (36) become small, as n increases. That is, the quantum fluctuations are successfully incorporated into the mean-field during the iterations. The above analytic and numerical results indicate clearly that the sign of $a^{(n)}b^{(n)}$ between two successive iterations is important whether or not the self-consistent CHF theory would be applicable.

IV. ANALYTIC CONDITIONS ON APPLICATIONS OF MEAN-FIELD THEORY

Since the analytic formulae within the two dimensional subspace discussed in the previous section nicely explain the characteristic feature of numerical iterative process of the CHF calculation near the level repulsive region, our next task is to explore what condition is there capable of estimating an existence of the mean-field. In the previous section, it is clarified that the CHF theory breaks down when the off-diagonal Hamiltonian $h_{A,A+1}^{(n)}$ changes its sign from iteration to iteration, whereas it is successfully applied when the sign is kept the same during the iteration. Namely, it is shown that the ratio of two successive off-diagonal components $h_{A,A+1}^{(n+1)}=h_{A,A+1}^{(n)}$, especially, the first relation $h_{A,A+1}^{(2)}=h_{A,A+1}^{(1)}$ plays a decisive role for an existence of the mean-field. That is, there exists a self-consistent mean-field, when there holds the condition

$$\frac{h_{A,A+1}^{(2)}}{h_{A,A+1}^{(1)}} = 0: \quad (37)$$

From the discussion in the previous section, it is easily shown that a sign of $h_{A,A+1}^{(n+1)}=h_{A,A+1}^{(n)}$ is always positive when the condition in Eq.(37) is satisfied, while it changes its sign from iteration to iteration when the condition is not satisfied.

In this section, we focus on discussing what is meant by the above condition. The ratio of two successive off-diagonal components satisfies a relation

$$\begin{aligned} \text{sign } \frac{h_{A,A+1}^{(n+1)}}{h_{A,A+1}^{(n)}} &= \text{sign } \frac{h_{A,A+1}^{(n+1)} = a^{(n)}b^{(n)}}{h_{A,A+1}^{(n)} = a^{(n)}b^{(n)}} \\ &= \text{sign } h_{A,A+1}^{(n+1)} = a^{(n)}b^{(n)}; \quad (38) \end{aligned}$$

because a sign of $h_{A,A+1}^{(n)}$ and that of $a^{(n)}b^{(n)}$ are always opposite, which is derived from our choice of states satisfying $\langle q_0 | q \rangle < \langle q_{A+1} | q \rangle$ and from the discussion based on the perturbation theory, and is justified by our numerical calculation. With the aid of Eq.(31), the last quantity in Eq.(38) is expressed as

$$\frac{h_{A,A+1}^{(n+1)}}{a^{(n)}b^{(n)}} = \frac{h_{A,A+1}^{(1)} + a^{(n)}b^{(n)}(v_{A+1;A,A+1} + 2wQ_{A,A+1}^2) + wb^{(n)}Q_{A,A+1}(Q_{A+1;A+1} - Q_{A;A})}{a^{(n)}b^{(n)}}: \quad (39)$$

Since an applicability of the mean-field is supposed to be decided by a competition between the quantum fluctuation (ph component of $h^{(1)}$) and the mean-field part (pp and hh components of $h^{(1)}$), let us find their relation by using the following relation

$$U^{(1)}h^{(1)}U^{(1)\dagger} = \begin{pmatrix} 1 & 0 \\ 0 & 1 \end{pmatrix}; \quad (40)$$

which should approximately hold within the truncated

space under the assumption in Eq. (25). From an off-diagonal component of the above relation, one gets

$$h_{A+1;A+1}^{(1)} - h_{A;A}^{(1)} = \frac{n}{d^{(1)}}C^{(1)} + \frac{b^{(1)}O}{a^{(1)}}h_{A,A+1}^{(1)}: \quad (41)$$

Inserting Eq. (33) for Eq.(41), one obtains the following relation

$$h_{A,A+1}^{(1)} = f_{A+1}(q_0) - a(q_0) + w(Q_{A+1;A+1} - Q_{A;A})g = \frac{C^{(1)}}{d^{(1)}} + \frac{b^{(1)}O}{a^{(1)}}h_{A,A+1}^{(1)}: \quad (42)$$

With the aid of Eq. (42), a quantity in Eq.(39) for the case with $n = 1$ is expressed as

$$\frac{h_{A,A+1}^{(2)}}{a^{(1)}b^{(1)}} = \frac{1}{b^{(1)2} - a^{(1)2}} \frac{a+1(q_0) - a(q_0) - (v_{A+1;A,A+1} + 2wQ_{A,A+1}^2)}{w(Q_{A;A} - Q_{A+1;A+1})O(b)}; \quad (43)$$

where the higher-order term containing a small parameter $b^{(1)}$ is written as

$$O(b) = -2b^{(1)2}v_{A+1;A,A+1} - 2wQ_{A,A+1}^2 + \frac{wb^{(1)}}{a^{(1)}}(1 - 2b^{(1)2}Q_{A,A+1}Q_{A+1;A+1} - Q_{A;A}): \quad (44)$$

Since a factor $(b^{(1)} - a^{(1)})$ is always negative (because there holds a relation $|a^{(1)}| > |b^{(1)}|$ in the unitary transformation in Eq.(27)), one finally gets a relation,

$$\begin{aligned} \text{sign } \frac{h_{A,A+1}^{(2)}}{h_{A,A+1}^{(1)}} &= \text{sign } \frac{h_{A,A+1}^{(2)}}{a^{(1)}b^{(1)}} \\ &= \text{sign } f_{A+1}(q_0) - f_A(q_0) - (v_{A+1,A,A+1} + 2wQ_{A,A+1}^2) \\ &\quad + w(Q_{A,A} - Q_{A+1,A+1}) + O(b); \end{aligned} \quad (45)$$

With the aid of the above relation, our condition (37) is expressed as

$$\begin{aligned} f_{A+1}(q_0) - f_A(q_0) &< v_{A+1,A,A+1} + 2wQ_{A,A+1}^2 \\ &\quad + w(Q_{A,A} - Q_{A+1,A+1}) + O(b); \end{aligned} \quad (46)$$

which guarantees an existence of the self-consistent mean field, whereas the opposite condition

$$\begin{aligned} f_{A+1}(q_0) - f_A(q_0) &> v_{A+1,A,A+1} + 2wQ_{A,A+1}^2 \\ &\quad + w(Q_{A,A} - Q_{A+1,A+1}) + O(b); \end{aligned} \quad (47)$$

states a breakdown of the mean-field. Here, it should be mentioned that a sign of the two-body interaction is important in Eqs.(46) and (47), which is in stark contrast with the well-known stability condition of the mean-field. Furthermore, the present condition on a breakdown of the mean-field has single-particle character, whereas the stability condition of the mean-field has collective character.

The physical meaning of the condition in Eq. (46) is clear: two-body correlation between nucleons can be successfully incorporated into the mean-field as much as possible when the energy difference between two interacting orbits is not smaller than the quantum fluctuations coming from the two-body residual interaction and quadrupole deformation.

Figure 7(a) gives the sp. energy difference between two specific orbits $f_A(q)$ and $f_{A+1}(q)$, and the quantum fluctuations which are the sum of $v_{A+1,A,A+1}$, $2wQ_{A,A+1}^2$ and $w(Q_{A,A} - Q_{A+1,A+1})$. In this figure and in Fig. 8, the q_0 -representation is used for any value of q in the convergent region, and $q(q_0)$ is numerically determined by the configuration dictated method. In the non-convergent region, the q_0 -representation is fixed at the critical point and is treated as a changeable parameter. Effects coming from the higher-order term $O(b)$ is neglected. Our numerical results clearly show how nicely the analytic condition in Eq. (46) does hold. Near the critical point, one may observe that the difference of sp. energies is almost equal to the quantum fluctuations, i.e., $f_{A+1}(q) - f_A(q) \approx v_{A+1,A,A+1} + 2wQ_{A,A+1}^2 + w(Q_{A,A} - Q_{A+1,A+1})$. Figure 7(b) shows the difference of sp. energies $f_{A+1}(q) - f_A(q)$, the two-body residual interaction $v_{A+1,A,A+1}$, and the effects from quadrupole deformation $2wQ_{A,A+1}^2 + w(Q_{A,A} - Q_{A+1,A+1})$, separately.

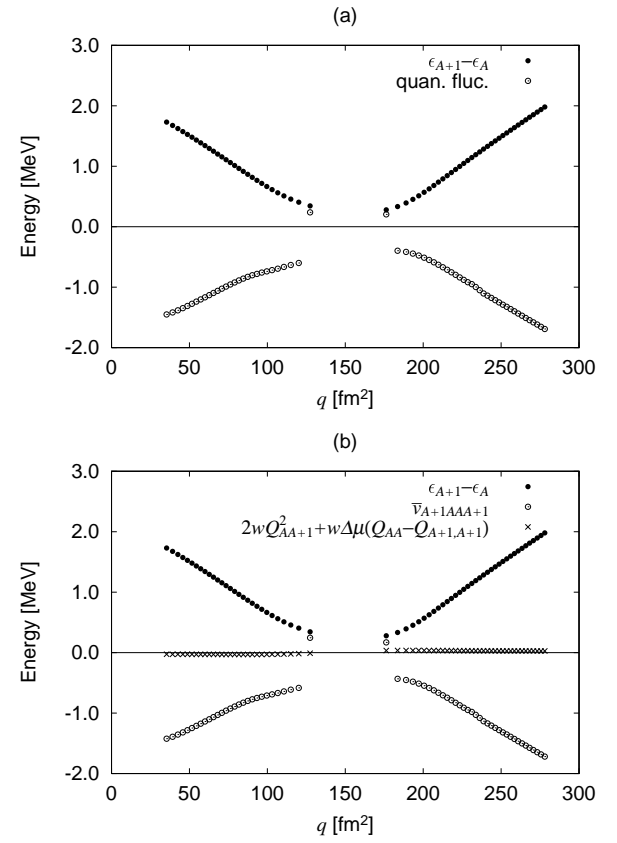


FIG. 7: (a) The energy difference between two specific orbits and quantum fluctuations as a function of quadrupole moment; (b) the sp. energy difference, two-body residual interaction and the sum of deformation fluctuation and quadrupole deformation.

One may observe that a competition between $v_{A+1,A,A+1}$ and the two-body residual interaction $v_{A+1,A,A+1}$ indeed plays a dominant role in determining whether or not the concept of CHF mean-field is realized.

Figure 8(a) depicts the ratio $h_{A,A+1}^{(2)} = h_{A,A+1}^{(1)}$ as a function of quadrupole parameter (since the average quadrupole moment q has no meaning in the non-convergent region). One may see that in the convergent region the ratio is always kept positive except for some exceptional points, where the deformation fluctuation between two specific orbits $Q_{A,A+1}$ is almost zero as shown in Fig. 8(b). Near the critical point, the ratio is going to reach zero. When one slightly decreases the deformation from the critical point, the ratio becomes negative where the CHF calculation meets a difficulty of non-convergence. After the non-convergent region, the ratio becomes positive, and the convergent state appears again. From these numerical calculation, it is clear that our condition in Eq. (37) actually works well in evaluating whether the concept of the mean-field is realized or not in the many-Fermion system.

At the end of this section, it should be remarked some comments on the exceptional points discussed above.

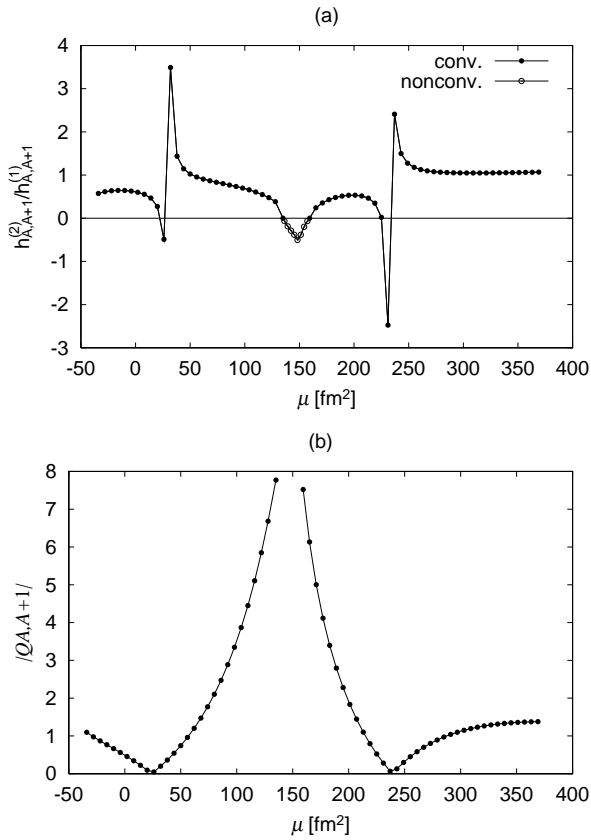


FIG. 8: (a) The ratio of off-diagonal components between the first and second iterations for each given state. Conv. and nonconv. stand for the convergent CHF states and non-convergent region; (b) the absolute value of off-diagonal quadrupole moment as a function of quadrupole parameter .

Since the ph component of the quadrupole operator $\mathcal{D}_{A,A+1,j}$ is almost zero, which just corresponds to a full alignment state created by the angular momentum constraint in the cranked HF theory, a new deformed state can not be generated by the quadrupole operator within the truncated two dimensional subspace. What actually happens at these exceptional points is an importance of the other part of the sp. space outside the two dimensional subspace spanned by $'_A(q_j)$ and $'_{A+1}(q_j)$. Since our simple analytic understanding by using the 2 2 Hamiltonian matrix does not work in this specific situation, an appearance of exceptional points is out of our present discussion.

V. SUMMARY

In the present work, the pairing correlation is not included. After including the pairing correlation, the sit-

uation so far discussed might become more complicated, because there are many dynamical competitions not only between the ph type two-body residual interaction and the HF potential, between the pp type two-body residual interaction and the pairing potential, but also their cross effects. Moreover, the two mean-fields characterized by different configurations are mixed up by the pairing correlation, and the uv factor introduced by the BCS theory makes a concept of the configuration obscure. Some numerical evidence on an applicability of the CHFB theory near level crossing region has been discussed in Ref. [13].

In summary, the non-convergent difficulty in level repulsive region is discussed analytically in the self-consistent mean-field theory. It turns out that the CHF mean-field breaks down when the quantum fluctuations coming from two-body residual interaction and quadrupole deformation become larger than an energy difference between two avoided crossing orbits. Deriving the analytic condition, we make it clear that the competition between one-body potential and quantum fluctuations mainly coming from two-body residual interaction plays an important role whether the self-consistent CHF mean-field is realized or not. However, the breakdown of the CHF mean-field at certain range of the quadrupole deformation q does not mean a necessity of introducing some quantum mechanical treatment, because the constrained operator \hat{Q} in the CHF theory is put in by hand. Furthermore, microscopic investigation is needed to answer the very interesting conclusion in Ref. [6] by introducing dynamical constrained operators based on the SCC method [29, 30] in the level crossing region.

Acknowledgments

This work is supported in part by the Japan Society for the Promotion of Science (JSPS) and the China National Natural Science Foundation (CNNSF) as the bilateral program between Japan and China. E.G. Zhao acknowledges the support by National Science Foundation of China under Grant No. 10375001, the China Major Basic Research Development Program under Grant No. G2000-0774-07, the Knowledge Innovation Project of the Chinese Academy of Sciences under Grant No. KJCX2-SW-N02.

[1] J. M. Arias, J. Dukelsky, and J. E. Garcia-Ramos, Phys. Rev. Lett. 91, 162502 (2003).

[2] R. Gonzalez-Ferez and J. S. Dehesa, Phys. Rev. Lett. 91,

113001 (2003).

[3] F. Intonti, V. Emilian, C. Lienau, T. Elsaesser, V. Savona, E. Runge, R. Zimmerman, R. Notzel, and K. H. Plobog, *Phys. Rev. Lett.* 87, 076801 (2001).

[4] C. Dembowski, H. D. Graf, H. L. Harney, A. Heine, W. D. Heiss, H. Rehfeld, and A. Richter, *Phys. Rev. Lett.* 86, 787 (2001).

[5] I. Hamamoto, *Nucl. Phys. A* 271, 15 (1976).

[6] R. Bengtsson and W. Nazarewicz, *Z. Phys. A* 334, 269 (1989).

[7] T. Bengtsson and I. Ragnarsson, *Nucl. Phys. A* 436, 14 (1985).

[8] R. Bengtsson, T. Bengtsson, M. Bergstrom, H. Ryde, and G. B. Hagemann, *Nucl. Phys. A* 569, 469 (1994).

[9] T. Bengtsson, *Nucl. Phys. A* 496, 56 (1989).

[10] A. Axelsson, R. Bengtsson, and J. Nyberg, *Nucl. Phys. A* 708, 226 (2002).

[11] A. Axelsson, R. Bengtsson, and J. Nyberg, *Nucl. Phys. A* 708, 245 (2002).

[12] K. Iwasawa, F. Sakata, Y. Hashimoto, and J. Terasaki, *Prog. Theor. Phys.* 92, 1119 (1994).

[13] L. Guo, F. Sakata, and E.-G. Zhao, *Nucl. Phys. A* 740, 59 (2004).

[14] L. Guo, F. Sakata, and E.-G. Zhao, *Phys. Rev. Lett.* (submitted).

[15] D. Gogny, in *Nuclear Self-Consistent Fields*, edited by G. Ripka and M. Pomeau (North-Holland, Amsterdam, 1975).

[16] J. Dachraoui and D. Gogny, *Phys. Rev. C* 21, 1568 (1980).

[17] M. Girod and B. Grammaticos, *Phys. Rev. C* 27, 2317 (1983).

[18] J. F. Berger, M. Girod, and D. Gogny, *Nucl. Phys. A* 428, 23c (1984).

[19] J. F. Berger, M. Girod, and D. Gogny, *Nucl. Phys. A* 502, 85c (1989).

[20] J. F. Berger, M. Girod, and D. Gogny, *Comput. Phys. Commun.* 63, 365 (1991).

[21] H. Flöck, P. Quentin, A. K. Kerman, and D. Vautherin, *Nucl. Phys. A* 203, 433 (1973).

[22] J. Dobaczewski, J. Dudek, S. G. Rohozinski, and T. R. Werner, *Phys. Rev. C* 62, 014310 (2000).

[23] J. Dobaczewski, J. Dudek, S. G. Rohozinski, and T. R. Werner, *Phys. Rev. C* 62, 014311 (2000).

[24] J. Dobaczewski and J. Dudek, *Phys. Rev. C* 52, 1827 (1995).

[25] H. Molique, J. Dobaczewski, and J. Dudek, *Phys. Rev. C* 61, 044304 (2000).

[26] W. Satula, J. Dobaczewski, J. Dudek, and W. Nazarewicz, *Phys. Rev. Lett.* 77, 5182 (1996).

[27] G. Hackman, R. Wadsworth, D. S. Haslip, R. M. Clark, J. Dobaczewski, J. Dudek, S. Libotte, and K. H. et al., *Phys. Rev. C* 52, R2293 (1995).

[28] G. Audi, O. Bersillon, J. Blachot, and A. H. Wapstra, *Nucl. Phys. A* 624, 1 (1997).

[29] T. Marumori, T. Marukawa, A. Kuriyama, and F. Sakata, *Prog. Theor. Phys.* 64, 1294 (1980).

[30] F. Sakata, T. Marumori, Y. Hashimoto, and S. W. Yan, *Suppl. Prog. Theor. Phys.* 141, 1 (2001).